Measurement of the V2I Massive Radio Channel with the MaMIMOSA Sounder in a Suburban Environment

D.P. Gaillot*†, P. Laly*, N. Dahmouni*, G. Delbarre*, M. Van den Bossche‡, G. Vermeeren‡, E. Tanghe‡, E.P. Simon*†, W. Joseph‡, L. Martens‡, M. Liénard*

*IEMN (UMR 8520), University of Lille, Villeneuve d'Ascq, France. martine.liénard@univ-lille.fr

†IRCICA (USR 3380), University of Lille, Villeneuve d'Ascq, France. davy.gaillot@univ-lille.fr

‡INTEC - WAVES, Ghent University, Ghent, Belgium. wout.joseph@ugent.be

***Abstract*—This paper presents the first V2I channel sounding campaign with the real-time massive MIMO radio channel sounder named MaMIMOSA. This equipment has been jointly developed by ULille (FR) and UGhent (BE) for 5G V2X applications. The system is equipped with a massive 64-antenna array for Tx whereas up to 16 individual antennas can be deployed for Rx. The MaMIMOSA hardware and software capabilities allow to freely adapting the sounding parameters to the investigated scenario demonstrating its versatility and flexibility. Radio channels were measured at 5.89 GHz with 80 MHz bandwidth at the ULille campus using with mean vehicle speed of 30 km/h. In addition to this suburban mobility scenario, Obstructed Line-Of-Sight static radio channels were collected for a roadside to parking setup to study the influence of vegetation. Very preliminary Doppler characteristics are reported from the measured radio channels.**

***Index Terms*—Massive MIMO channel sounding, V2X, propagation, measurements.**

I. Introduction

In our modern world where mobile connectivity has become a necessity for many network users, there is a need for technological advances and computer abilities to provide faster, smarter and safer wireless networks [1]. The upcoming 5G NR (New Radio) being currently defined by 3GPP [2], [3] is expected to reach larger data rates with improved networks efficiency compared to previous legacy standards such as 4G LTE. Moreover, it widens its original radio mobile domain of application by including machines in industrial setups, vehicular communications (Vehicle-to-Everything or V2X) [4] and smart cities [5], [6]. These use cases encompass three fundamentally different dimensions: enhanced mobile broadband (eMBB), massive machine type communications (mMTC) and ultra-reliable low latency communications (URLLC). Among novel technologies expected to deliver the promised specifications of 5G NR, Massive MIMO [7] and the use of larger bandwidths at millimeter wave (mmW) frequencies are the most widely investigated in the research community. Massive MIMO is an asymptotic extension of multi-user MIMO (MU-MIMO) where the number of transmitting antennas is very large compared to previous MIMO techniques. This enables simultaneously serving many user equipment (UE) within the same frequency-time slot even if they generally are equipped with one antenna [8], [9]. Early works such as [10], [11] present the fundamental information, theoretical aspects as well as limits of the massive MIMO technology.

Beyond the fact that the main benefits envisioned by massive MIMO must be evaluated (e.g. reduction in latency on the air interface, multiple-layer access simplification or even robustness to undesired or intentional jamming [12]), legacy propagation models used in network planning tools must be revisited accordingly. Furthermore, the wide-sense stationarity (WSS) uncorrelated scattering (US) assumption WSSUS [13] of the channel are not often verified in realistic dynamic environments from the Tx array side. The violation of the WSSUS assumptions which can happen in practice in vehicular scenarios [14] avoid a simplified statistical description of channels. It follows real-time massive MIMO systems must be used to assess the WSSUS assumptions and is a requisite to grasp the time-varying spatial characteristics of the radio channel. This approach can be rather cost-expensive due to the architecture complexity [15] resulting in RF impairments or synchronization issues between the massive array and the UEs.

To this end, a real-time 64 x 16 massive MIMO radio channel sounder operating between 2 and 12 GHz with 80 MHz bandwidth has been jointly developed by the University of Lille (France) and Ghent (Belgium) for 5G mobility scenarios such as V2X communications [16]. The architecture relies on the physical and reconfigurable software radio channel sounder MIMOSA (MIMO Sounding Architecture) [17]. MaMIMOSA (Massive MIMOSA) has been designed to fulfill all the constraints identified in time-varying massive MIMO channels such as high Doppler resolution with a large Doppler span, spatial antenna selection, compactness, energy consumption, etc. The sounding parameters of the developed massive system can be freely selected depending on the studied environment resulting in the measured massive MIMO radio channel without the need for additional tedious post-processing. The MaMIMOSA antenna array is a 10 x 10 vertical planar antenna array built by the University of Ghent. 64 elements of the array are SMA-connected to the Tx unit using coaxial cables

whereas the 36 remaining antennas at the perimeter are used as dummies to attenuate the finite array side effects.

In this work, MaMIMOSA was setup to perform up to 64 x 8 radio channel measurements at 5.89 GHz with 80 MHz bandwidth for V2I communications. In a first set of measurements, 64 x 1 time-varying radio channels were assessed on the scientific campus of the University of Lille with mean vehicle speed of 30 km/h and Non Line-Of-Sight/Line-Of-Sight (NLOS/LOS) shadowing condition. In a second set, static Obstructed LOS (OLOS) 64 x 8 radio channels were measured between the transmitter located on the roadside and receiver on an adjacent parking lot to study the influence of vegetation. Since the campaign is very recent, only an early analysis of the RMS delay spread, received SNR and Doppler/speed characteristics were evaluated from the measured channels and presented in this paper. Nonetheless, the results show that those characteristics are highly uniform across the massive antenna array with no masking effects. Also, due to lack of space, the vegetation study will be presented during the conference. Nonetheless, The campaign already highlights the potential of MaMIMOSA to faithfully grasp the main characteristics of radio channels which can be subsequently used for developing realistic massive MIMO radio channel models.

II. MaMIMOSA Frame structure

Two frame structures, *streaming* and *streamshot*, have been designed in MaMIMOSA. They can be selected depending upon the time-varying nature of the radio channel and associated parameters that are investigated by the user. These two modes are described in the following paragraphs.

A. Streaming mode for time-varying scenarios

When a scenario with large mobility is considered like for V2X communications, the MaMIMOSA *streaming* mode is selected. It is associated with the frame structure illustrated in Fig. 1(a). Each frame consists in one 51.2 μs preamble subsequently followed by 128 blocks of 8 OFDM symbols. Each symbol corresponds to a row of the 8 x 8 massive array (8 x 16 radio channel) and has a duration of 121.92 μs including the cyclic prefix. Each symbol is simultaneously measured over the 16 receiving antennas. The whole array is spanned by sequentially switching between the 8 rows. Hence, a single 64 x 16 massive MIMO matrix (or block) is measured in $\sim$1 ms and the frame duration is $\sim$125 ms. Hence, the maximum Doppler span is $\pm$ 512 Hz (93 km/h maximum speed) with 8 Hz Doppler resolution. The preamble provides the time synchronization of the frame required to decode the OFDM symbols. Each OFDM symbol corresponds to an 8-antenna subarray out of 64. The time duration between consecutive frames was manually set to 500 ms. The total number of transmitted OFDM subcarriers per symbol N_t is 8192 which can be uniformly distributed on each antenna element using interleaved OFDM. For instance, the frequency space δF between the subcarriers of a single antenna is 97.66 kHz, meanwhile the frequency space of between subcarriers is 12.21 kHz. The automatic gain control (ACG) is performed with the cyclic prefix for each symbol and is used to correct the measured MIMO matrix. The reader is encouraged to read the following references to learn more about MaMIMOSA's architecture and signal processing [16], [17]. The non-stationary fading process of vehicular channel can be characterized by assuming local stationarity for a finite region in time and frequency. We reported in a recent work a stationarity time of 567 ms for the same scenario at 1.35 GHz [14] and similar speeds. Hence, it is assumed that the measurement time used to obtain the estimates of the Doppler and delay spreads are within the stationarity region.

B. Streamshot mode for static scenarios

When the time-variation of the radio channel is not the purpose of the measurement or simply because the radio channel is supposed to be static in nature, the *streamshot* mode of MaMIMOSA can be selected and is associated the frame structure illustrated in Fig. 1(b). Each frame consists in one 51.2 μs preamble subsequently followed by a single block of 8 121.92 μs OFDM symbols including the cyclic prefix. The total frame duration to measure a single 64 x 16 massive MIMO matrix is $\sim$1 ms. The time duration between consecutive frames was also manually set to 50 ms. Since time-synchronization is performed to measure a single radio channel, the Doppler information is lost. However, this mode relaxes the streaming and processing constraints within the FPGA to the hard drive in contrast to the *streaming* mode.

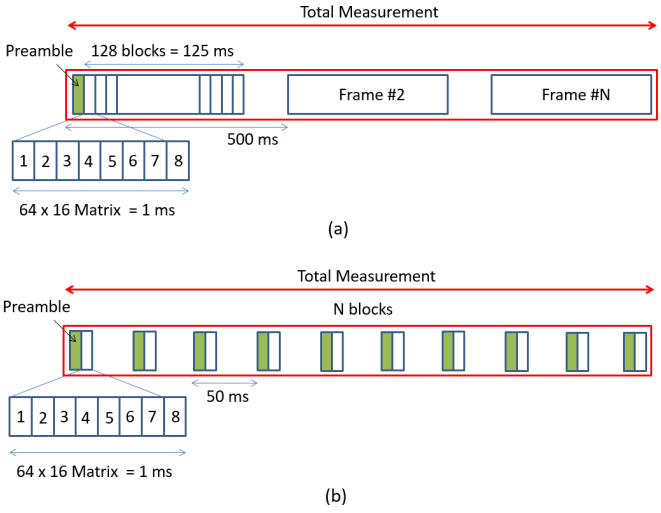

Fig. 1. MaMIMOSA frame structure for (a) *streaming* and (b) *streamshot* mode.

III. Measurement campaign description

The massive 64-antenna array was placed on a tripod at same location on the sidewalk during the whole measurement campaign. The emitted power per RF chain was set to 0 dBm during the whole measurement campaign knowing that the maximum power per RF chain is 30 dBm.

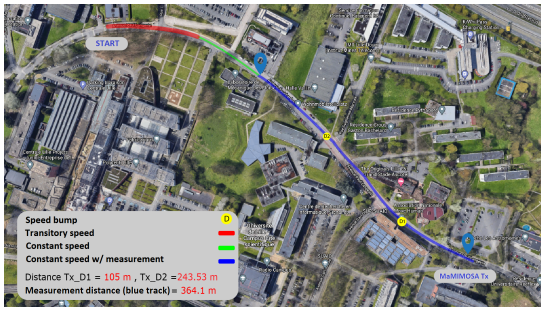

Fig. 2. schematic top view of the V2I measurement campaign at the ULille campus.

Fig. 3. Picture from the rear side of the Tx array with the van completing its drive test. The Rx antenna is one of the 8 antennas located on the van rooftop.

A. *V2I scenarios*

Figure. 2 depicts a schematic top view of the V2I measurement campaign at the ULille campus. Tx was placed such that its main radiating lobe was parallel to the main boulevard. The single receiver antenna Rx was placed on a van rooftop and is the same as the elementary antenna of the array. The van performed a drive test along the boulevard with an averaged speed of 30 km/h toward Tx. The radio channel was measured during 89 frames with the *streaming* mode for a total recording time of ∼45 seconds. Figure. 3 presents a picture from the rear side of the Tx array with the van completing its drive test.

B. *Static scenarios*

In addition, Figure. 4 depicts a picture of the 4 OLOS measurement scenarios between the Tx array (located at same place than for the V2I scenario) and 8-antenna Rx array. Tx array was facing the building. The measurement recently took place at the end of the summer such that the foliage of the trees separating the sidewalk and parking was dense. The radio channel was measured during 236 frames with the *streamshot* mode. The results of this study will be presented during the conference due to the lack of space in the manuscript.

IV. RMS Delay spread, SNR, and Doppler characteristics

Beforehand, and based on the measurement scenario, the first 55 frames were identified as NLOS and then LOS until the end. First, Fig. 5 presents the SNR estimated from the radio channels as a function of the number of frames and massive array antenna index. As expected, the received SNR increases

Fig. 4. Schematic top view of the 4 OLOS static measurement positions. The green triangle corresponds to the Tx position on the sidewalk behind the trees observable by their shadows on the ground.

as the van is getting closer to the massive array. Large fading occurring in the LOS area is due to the ground reflection. The results indicate that the received SNR is uniform (with deviation < 3 dB) across the array highlighting the fact that no major masking effects took place during the campaign for this scenario. Furthermore, it shows the capability of MaMIMOSA to faithfully measure the radio channel characteristics. Then, Fig. 6 presents the RMS delay spread (computed with 20 dB threshold) estimated from the power delay profiles averaged across all antennas as a function of Tx - Rx distance. The results indicate that the delay spread values decrease gradually from 400 ns to 20 ns as the van is getting closer to the emitter. Since the received SNR is low at the beginning of the drive-test, the large spread values mostly correspond to the noise background. Nonetheless, as the van approaches the massive array, the scenario becomes mostly LOS with low delay spread values.

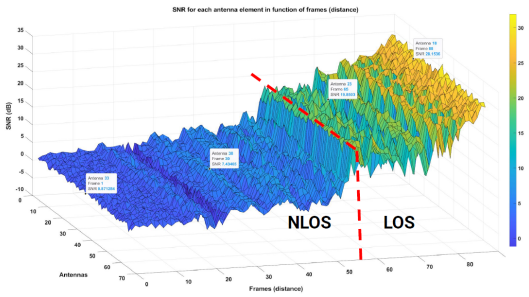

Fig. 5. Estimated SNR as a function of the number of frames (Tx - Rx distance) and antenna index.

The estimated Delay-Doppler profile is shown in Figure. 7 as a function of Tx - Rx distance for frame #70 and Tx antenna #40 as an arbitrary example. The spectrum indicates the presence of several multipath components with similar Doppler shift values as the principal Doppler shift due to the

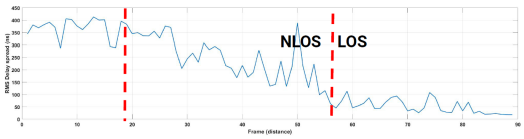

Fig. 6. Estimated RMS delay spread as a function of the number of frames (Tx - Rx distance).

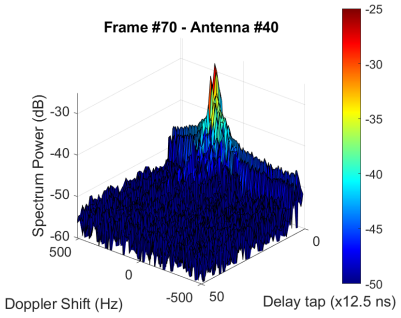

Fig. 7. Example of estimated Delay-Doppler spectrum for frame #70 and Tx antenna 40.

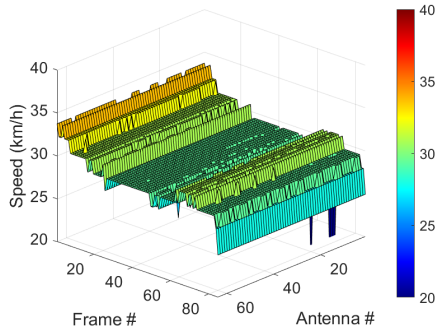

Fig. 8. Speed (in km/h) as a function of the number of frames (i.e. Tx - Rx distance) and massive array antenna position.

van. In addition, Fig. 8 presents the estimated speed measured for the V2I scenario as a function of the number of frames (Tx - Rx distance) and massive array antenna index. The associated vehicle speed computed as the maximum in the Doppler spectrum for each frame (i.e. most energetic multipath) is in good agreement with the 30 km/h speed maintained during the measurement. Similarly to the SNR results, it can be observed that the speed is uniform across the array for all frames despite the scenario evolving from NLOS to LOS with no masking effects. Furthermore, this high degree of correlation between antennas indicate that modeling of the massive MIMO radio channel can be simplified for this scenario.

V. Conclusion

In this contribution, the real-time 64 x 16 massive MIMO sounder called MaMIMOSA based on space-frequency division multiplexing and antenna subarray switching has been used for a NLOS/LOS measurement campaign at 5.89 GHz with 80 MHz bandwidth on the University of Lille Campus using different Massive transmitter-receiver configurations with mean vehicle speed of 30 km/h. In addition, the influence of vegetation was investigated thanks to the measurement of OLOS static radio channels from the roadside to a parking lot. The RMS delay spread, SNR and Doppler characteristics were evaluated from the measured radio channels and are shown to agree well with the campaign configuration and shadowing condition. For instance, it is shown that the received SNR and Doppler shift values are highly uniform across the massive array indicating no masking effects and, therefore, a high degree of correlation between antennas.

Acknowledgment

This work was supported through the OS4 SMARTIES research program by the ELSAT2020 project co-financed by the European Union with the European Regional Development Fund, the French state, and the Hauts-de-France Region Council.

References

[1] I. F. Akyildiz, S. Nie, S.-C. Lin, and M. Chandrasekaran, "5g roadmap: 10 key enabling technologies," *Computer Networks*, vol. 106, pp. 17 – 48, 2016. [Online]. Available: http://www.sciencedirect.com/science/article/pii/S1389128616301918

[2] S. Parkvall, E. Dahlman, A. Furuskar, and M. Frenne, "Nr: The new 5g radio access technology," *IEEE Communications Standards Magazine*, vol. 1, no. 4, pp. 24–30, Dec 2017.

[3] 3GPP, *3GPP Technical Report Technical Specification Group Radio Access Network; Study on NR Industrial Internet of Things (IoT), Release 16*, 2015.

[4] D. Phan-Huy, M. Sternad, and T. Svensson, "Making 5g adaptive antennas work for very fast moving vehicles," *IEEE Intelligent Transportation Systems Magazine*, vol. 7, no. 2, pp. 71–84, Summer 2015.

[5] A. Osseiran, F. Boccardi, V. Braun, K. Kusume, P. Marsch, M. Maternia, O. Queseth, M. Schellmann, H. Schotten, H. Taoka, H. Tullberg, M. A. Uusitalo, B. Timus, and M. Fallgren, "Scenarios for 5g mobile and wireless communications: the vision of the metis project," *IEEE Communications Magazine*, vol. 52, no. 5, pp. 26–35, May 2014.

[6] A. Gupta and R. K. Jha, "A survey of 5g network: Architecture and emerging technologies," *IEEE Access*, vol. 3, pp. 1206–1232, 2015.

[7] T. L. Marzetta, "Noncooperative cellular wireless with unlimited numbers of base station antennas," *IEEE Transactions on Wireless Communications*, vol. 9, no. 11, pp. 3590–3600, November 2010.

[8] N. B. Labs., *5G New Radio (NR) : Physical Layer Overview and Performance.*, 2018. [Online]. Available: http://ctw2018.ieee-ctw.org/files/2018/05/5G-NR-CTW-final.pdf

[9] K. Technologies., *Field Testing in 5G NR.*, 2018. [Online]. Available: https://literature.cdn.keysight.com/litweb/pdf/5992-3299EN.pdf

[10] E. Björnson, J. Hoydis, M. Kountouris, and M. Debbah, "Massive mimo systems with non-ideal hardware: Energy efficiency, estimation, and capacity limits," *IEEE Transactions on Information Theory*, vol. 60, no. 11, pp. 7112–7139, Nov 2014.

[11] J. Jose, A. Ashikhmin, T. L. Marzetta, and S. Vishwanath, "Pilot contamination and precoding in multi-cell tdd systems," *IEEE Transactions on Wireless Communications*, vol. 10, no. 8, pp. 2640–2651, August 2011.

[12] E. G. Larsson, O. Edfors, F. Tufvesson, and T. L. Marzetta, "Massive mimo for next generation wireless systems," *IEEE Communications Magazine*, vol. 52, no. 2, pp. 186–195, February 2014.

[13] P. Bello, "Characterization of randomly time-variant linear channels," *IEEE Transactions on Communications Systems*, vol. 11, no. 4, pp. 360–393, 1963.

[14] M. Yusuf, E. Tanghe, F. Challita, P. Laly, D. Gaillot, M. Lienard, L. Martens, and W. Joseph, "Stationarity analysis of v2i radio channel in a suburban environment," *IEEE Transactions on Vehicular Technology*, pp. 1–1, 2019.

[15] J. Vieira, S. Malkowsky, K. Nieman, Z. Miers, N. Kundargi, L. Liu, I. Wong, V. Öwall, O. Edfors, and F. Tufvesson, "A flexible 100-antenna testbed for massive mimo," in *2014 IEEE Globecom Workshops (GC Wkshps)*, Dec 2014, pp. 287–293.

[16] P. Laly, D. P. Gaillot, G. Delbarre, M. V. d. Bossche, G. Vermeeren, F. Challita, E. Tanghe, E. P. Simon, W. Joseph, L. Martens, and M. Liénard, "Massive radio channel sounder architecture for 5g mobility scenarios: Mamimosa," in *2020 14th European Conference on Antennas and Propagation (EuCAP)*, 2020, pp. 1–5.

[17] P. Laly, D. P. Gaillot, M. Lienard, P. Degauque, E. Tanghe, W. Joseph, and L. Martens, "Flexible real-time mimo channel sounder for multidimensional polarimetric parameter estimation," in *2015 IEEE Conference on Antenna Measurements Applications (CAMA)*, Nov 2015, pp. 1–3.